CELL CYCLE
2019, VOL. 18, NO. 9, 1019–1032
https://doi.org/10.1080/15384101.2019.1609830

Taylor & Francis
Taylor & Francis Group

RESEARCH PAPER

A novel function of anaphase promoting complex subunit 10 in tumor progression in non-small cell lung cancer

Yanan Wang[a,b], Tianyu Han[c], Mingxi Gan[b], Meng Guo[b], Caifeng Xie [b], Jiangbo Jin[a], Song Zhang[a], Pengcheng Wang[a], Jiaqing Cao[d], and Jian-Bin Wang[b]

[a]School of Life Sciences, Nanchang University, Nanchang City, Jiangxi, China; [b]School of Basic Medical Sciences, Nanchang University, Nanchang City, Jiangxi, China; [c]Department of Respiration, The First Affiliated Hospital of Nanchang University, Nanchang City, Jiangxi, China; [d]Department of Gastrointestinal Surgery, the Second Affiliated Hospital of Nanchang University, Nanchang City, Jiangxi, China

ABSTRACT

The anaphase promoting complex/cyclosome (APC/C), a cell cycle-regulated E3 ubiquitin ligase, is responsible for the transition from metaphase to anaphase and the exit from mitosis. The anaphase promoting complex subunit 10 (APC10), a subunit of the APC/C, executes a vital function in substrate recognition. However, no research has reported the connection between APC10 and cancer until now. In this study, we uncovered a novel, unprecedented role of APC10 in tumor progression, which is independent of APC/C. First, aberrant increase of APC10 expression was validated in non-small cell lung cancer (NSCLC) cells and tissues, and the absence of APC10 repressed cell proliferation and migration. Of great interest, we found that APC10 inhibition induced cell cycle arrest at the G0/G1 phase and reduced the expression of the APC/C substrate, Cyclin B1; this finding is different from the conventional concept of the accumulation of Cyclin B1 and cell cycle arrest in metaphase. Further, APC10 was found to interact with glutaminase C (GAC), and the inhibition of APC10 weakened glutamine metabolism and induced excessive autophagy. Taken together, these findings identify a novel function of APC10 in the regulation of NSCLC tumorigenesis and point to the possibility of APC10 as a new target for cancer therapy.

ARTICLE HISTORY
Received 21 September 2018
Revised 26 March 2019
Accepted 29 March 2019

KEYWORDS
APC10; GAC; glutamine metabolism; autophagy; NSCLC

Introduction

Autophagy, an evolutionarily conserved cellular process, catabolizes cytoplasmic proteins and damaged organelles to maintain cellular homeostasis [1,2]. A low level of basal autophagy is required for cells to sustain the normal turnover of cellular proteins and organelles [3]. In regard to cancer, autophagy plays a dual role; it either functions in tumor suppression or tumor progression [4]. In the presence of amino acids, autophagy is repressed through signaling of the mammalian target of rapamycin complex 1 (mTORC1), in which the mTORC1 complex interacts with the Unc-51-like kinase 1 (ULK1) kinase complex and directly phosphorylates the ULK1 subunits to inhibit ULK1 kinase activity [5–9]. During amino acid starvation, mTORC1 signaling is repressed and autophagy is induced to provide amino acids for cell survival [10,11]. Glutaminase, the first and the rate-limiting enzyme in glutaminolysis, is crucial for glutamine metabolism. Glutaminase C (GAC), an important isoform of glutaminase, has been demonstrated to be crucial for cancer initiation and progression [12–14]. When glutamine metabolism is abolished by inhibiting GAC, mTORC1 signaling is repressed, leading to the induction of autophagy [15].

The anaphase promoting complex/cyclosome (APC/C) is a cell cycle-regulated multimeric E3 ubiquitin ligase assembled from 13 individual subunits [16,17]. APC/C assembles polyubiquitin chains on substrates for destruction by the 26S proteasome [18]. APC/C activity needs two coactivators, cdc20 and cdh1, which interact with the APC/C and control different parts of the cell cycle [19]. APC/C-cdc20 targets both securin and Cyclin B1 for destruction, resulting in the metaphase-anaphase transition. APC/C-cdh1 also regulates the exit from mitosis and the maintenance of early G1 phase [20–22]. In addition to its role in the cell cycle, APC/C also has cell cycle-

CONTACT Jian-Bin Wang jianbinwang1@gmail.com; Jiaqing Cao cao.jiaqing@163.com
Supplemental data for this article can be accessed here.

independent functions. It was reported that a new centrosome-dependent activity of APC/C-cdc20 could control the morphogenesis of dendrites [23]. A previous study proposed that APC/C-cdh1 could regulate the bioenergetic and antioxidant status of neurons by degrading the key glycolytic enzyme PFKFB3 (6-phosphofructo-2-kinase/fructose-2,6-bisphosphatase-3) [24]. The APC/C is also involved in cancer progression. Many studies have proposed that chemical inhibition of APC/C is a potential therapeutic strategy in cancer [25–28]. In human primary multiple myeloma cells, the APC/C small molecule inhibitor proTAME induced the accumulation of Cyclin B1 and cell cycle arrest in metaphase [29]. A recent study found that inactivation of cdc20 resulted in replicative stress, cell cycle arrest and cell death, suggesting that APC/C-cdc20 is a promising target for anti-cancer therapy [30]. The anaphase promoting complex subunit 10 (APC10) is a core subunit of APC/C that is highly conserved in humans [31]. APC10 genetically and physically interacts with a series of subunits of the APC/C [32] and is necessary for the ubiquitination activity of APC/C by enhancing the affinity of the APC/C for its substrate [33,34]. Mutation of APC10 decreased the affinity of APC/C for its substrate [35,36]. These studies support the notion that APC10 plays an indispensable role as an APC/C subunit, but the role of APC10 independent of the APC/C remains unknown. In this study, we found an unexpected role in non-small cell lung cancer (NSCLC) cells that was independent of the APC/C. APC10 was overexpressed in NSCLC cell lines compared to human bronchial epithelial cell lines. APC10 was shown to interact with GAC; knocking down APC10 downregulated glutamine metabolism to induce autophagy, resulting in effective inhibition of the proliferation and migration of NSCLC cells.

Materials and methods

Reagents

Chloroquine (CQ) and DMSO were bought from Sigma (C7698, D2650). Thymidine and nocodazole were purchased from MedChemExpress (MCE, HY-N1150, HY-13520). Four percent polyformaldehyde was obtained from Solarbio (Solarbio, P1110). The APC10 (base:A^{483}-G, A^{486}-C, A^{489}-G, G^{492}-A) mutant plasmid was purchased from Tsingke. The antibody against APC10 was ordered from OriGene (TA319413). The mouse anti-β-actin antibody was purchased from Proteintech (66009–1-lg). The mouse anti-HA monoclonal antibody was ordered from Thermo Fisher Scientific (26,183). The rabbit polyclonal antibodies anti-LC3B, anti-ULK1, anti-CDC25A, anti-V5, anti-RB1, anti-CDK1, anti-CDC25C, anti-Cyclin B1, anti-VDAC, anti-GAPDH and anti-TBP were purchased from Proteintech (18725–1-AP, 20986–1-AP, 55031–1-AP, 14440–1-AP, 10048–2-Ig, 19532–1-AP, 16485–1-AP, 55004–1-AP, 10866–1-AP, 60004–1-Ig, 22006–1-AP). The rabbit polyclonal antibodies anti-ULK1 (phospho S758) and anti-GAC were purchased from Abcam (ab156920, ab93434).

Cell culture

The NSCLC cell lines A549, H1299, H358, H292 and SPC-A1 were purchased from ATCC and cultured in RPMI 1640 (Invitrogen, C11875500BT) medium supplemented with 10% fetal bovine serum (FBS) (Excell, FCS100). Human bronchial epithelial (HBE) cells were cultured in airway epithelial cell basal medium supplemented with bronchial/tracheal epithelial cell growth kit (ATCC). Human bronchial epithelial Beas-2b cells were purchased from ATCC and cultured in Dulbecco's modified Eagle medium (DMEM, high glucose; HyClone, SH30022.01B) supplemented with 10% FBS. All cells were cultured at 5% CO_2 at 37°C.

Patient samples

Fresh samples of human non-small cell lung cancer and paired normal tissues were kindly provided by Dr. Bentong Yu in the Department of General Surgery from the First Affiliated Hospital of Nanchang University. All samples were collected with patients' informed consent. Samples were immediately frozen and stored at -80℃ prior to western blot analyses.

DNA constructs

Human APC10 expression plasmid was constructed by PCR with the following primers: 5′-GCGAATTCGGATGACTACACCAAACAAGA-C-3′ (forward) and 5′-GCGGTACCTCACCTTAT TGAACGATACA-3′ (reverse). The construct was cloned into the pCMV-HA vector using the restriction enzymes EcoRI and KpnI and verified by sequencing.

MTT assay

Cells were seeded in 96-well plates at 5000 cells per well in 200 µl medium supplemented with 10% FBS for 24 h. Then, the cells were treated with autophagy inhibitor CQ at a final concentration of 20 µM for 48 h. The cells were next treated with 20 µl MTT (5 mg/ml) solution and incubated for 4 h at 37°C with 5% CO_2. Then, the culture medium was removed and 150 µl DMSO was added to each well, and the cells were incubated on an end-over-end shaker for 20 min. Finally, the absorbance at 570 nm was measured. Measurements were done in triplicate.

Scratch wound healing assay and transwell migration assay

For the scratch wound healing assay, the cells were seeded in 6-well plates to form a confluent monolayer of 80–90% confluence. Then, a straight line was drawn across the monolayer using 200 µl pipet tips. After washing the wells three times with PBS, fresh medium with 1% FBS was added, and the initial lines were photographed using a microscope (Olympus, IX71). Additional photos were taken at the indicated time points.

The transwell migration assay was performed using 8 µm pore size transwell chambers (Corning, 27117026). A total of 10^5 cells in 0.2 ml medium containing 1% FBS was seeded in the upper chambers. 500 µl RPMI 1640 supplemented with 10% FBS was added in the lower chamber of the transwell device. After incubation at 37°C for 10 h, the cells on the upper surface of the membrane were removed. Those on the lower surface of the membrane were fixed with 4% formaldehyde for 30 min; then the cells were stained with 2% crystal violet for 15 min and washed with 1× PBS until the water was clear. Finally, the cells were photographed using a microscope (Olympus, IX71).

Crystal violet staining, colony formation assay and saturation density assay

For the crystal violet staining assay, 3000 cells per well were seeded in 24-well plates in 500 µl of RPMI 1640 supplemented with 10% FBS. The medium was changed every other day. At the appointed times, the cells were fixed with 4% formaldehyde for 30 min and then stained with 2% crystal violet. Then, the crystal violet was removed, and 10% acetic acid was added. The dyes were extracted, and the relative proliferation was determined by measuring the absorbance at 595 nm.

For the colony formation assay, 500 cells per well were cultured in 6-well plates in RPMI 1640 supplemented with 10% FBS. The medium was changed every other day. After 10 days, the cells were fixed with 4% formaldehyde and then stained with 2% crystal violet. Images were obtained using a digital camera (Canon, EOS70D).

For the saturation density assay, 10^5 cells per well were cultured in 12-well plates in RPMI 1640 supplemented with 10% FBS. The medium was changed every other day. After 6 days, the cell number was counted.

Gene overexpression and knockdown

For gene overexpression, the cells were transfected with the indicated plasmids using the SuperFectin DNA Transfection Reagent kit (Pufei, 2102–100), and the transfection efficiency was determined by western blot using the relevant antibodies.

For gene knockdown, siRNAs that target APC10 (HSS115911, HSS173597, HSS173598) were purchased from Thermo Fisher (Cat. #1299001). HSS115911 and HSS173597 were used for knocking down APC10. The indicated siRNAs or Stealth RNAi^{TM} siRNA Negative Control from Thermo Fisher Scientific were transiently transfected into NSCLC cell lines using Superfectin II In Vitro siRNA Transfection Reagent (Pufei, 2103–100). The knockdown efficiency was determined by western blot using the relevant antibodies.

RNA purification and Q-PCR analysis

Total RNA of the NSCLC cell lines was extracted using TRIzol reagent (Invitrogen, 15596–026). The cDNA was synthesized using the Prime Script RT reagent kit with gDNA Eraser (Takara, RR047A). Q-PCR experiments were conducted using SYBR Green Premix Ex Taq II kit (Takara, RR820A). The relative amount of mRNA expression of target genes was calculated using the comparative Ct method and glyceraldehyde-3-phosphate dehydrogenase (GAPDH) as a control. The data were acquired using an ABI Vii ATM 7 Real-Time PCR System instrument. All Q-PCR reactions were performed in triplicate.

Immunoprecipitation and western blot

NSCLC cells were lysed in NP-40 buffer (20 mM Hepes, pH 7.4, 150 mM NaCl, 20 mM β-glycerol phosphates, 1 mM Na orthovanadate, 20 mM NaF, 0.5% Nonidet P-40) supplemented with PMSF (Dingguo, WB0181). Then, the cell lysates were centrifuged at 10,000 × g for 20 min at 4°C. The supernatants were precleared with protein G agarose beads (Roche, 11243233001) for 1 h at 4°C. Then, the supernatants were combined with the indicated antibodies supplemented with protein G agarose beads to incubate overnight at 4°C. On the second day, the immunocomplexes were washed with lysis buffer. The supernatants were suspended with 2× loading buffer and boiled for 10 min.

For western blotting, the proteins were subjected to 10% SDS-PAGE and then transferred to a PVDF membrane (Millipore, IPVH00010). After blocking with 5% skim milk (BD, 232100) at room temperature for 1 h, the membranes were incubated with the indicated antibodies overnight at 4°C. On the follow day, the membranes were washed 3 times at room temperature with 1× TBST for 10 min each time and incubated with secondary antibody at room temperature for 1 h. After being washed 3 times at room temperature with 1× TBST, the membranes were stained with ECL western blot detection reagent (TIANGEN, PA112-01). Proteins were then visualized using a digital gel image analysis system (TANON 5500).

Cell cycle synchronization

We followed the thymidine- and nocodazole-based (Thy-Noc) synchronization protocol [37]. The cells were seeded and attached by incubating 6-well plates with 2 ml medium supplemented with 10% FBS at 37°C in a humidified atmosphere with 5% CO_2 for 24 h. For the thymidine block, a 200 mM thymidine stock solution was prepared by dissolving 145.2 mg thymidine powder in 3 mL H_2O (or equivalent amounts) and sterilizing the solution by filtration through a 0.2 μm pore size filter. Slight warming can help to dissolve the thymidine. Then, 20 μl of the freshly prepared 40 mM stock was added to each 6-well plate (final concentration 2 mM). The cells were incubated with thymidine in a humidified atmosphere with 5% CO_2 at 37°C for 20 h. To release the cells from the thymidine block, the thymidine-containing growth medium was removed in the afternoon of the following day; the cells were washed twice with prewarmed 1× PBS, and 2 ml of complete medium was added to each 6-well plate. The cells were incubated for 5 h at 37°C in a humidified atmosphere with 5% CO_2. For mitotic cell arrest, we added nocodazole to a final concentration of 50 ng/ml. A stock solution was prepared by dissolving nocodazole powder in DMSO (e.g. 5 mg/ml) and stored frozen at -20°C. Cells were incubated with nocodazole for no longer than 10–11 h at 37°C in a humidified atmosphere with 5% CO_2. The cells were released from nocodazole-mediated arrest in early M phase.

Cell cycle analysis

The cells were seeded in 6-well plates with each treatment. Then, the cells were harvested and washed with 1× PBS, and 70% alcohol in PBS was added to the cells on ice for 2 h; the cells were washed with 1× PBS and resuspended with 400 μl guava cell cycle reagent (Millipore, 4700–0160) (PI:585/29). After incubation at 37°C for 15 min, the cells were analyzed using a BD FACS Jazz™ Cell Sorter (Becton Dickinson).

Immunofluorescence staining

The cells were cultured in 24-well plates for 18–24 h. Then, the cells were fixed with methanol

at room temperature for 20 min and washed with 1 × PBS three times. After adding 0.1% Triton X-100 (Sigma T8787-50) in PBS and incubating at room temperature for 5 min, the cells were blocked with 2.5% BSA in PBS for 1 h at room temperature. The cells were then incubated with the indicated antibodies for 1 h at room temperature. After rinsing with 1 × PBS, the cells were incubated with the indicated rhodamine-conjugated secondary antibody (Proteintech) for 1 h at room temperature in the dark. Then, the cells were washed with 1× PBS three times and mounted with DAPI Fluoromount-G mounting medium (SouthernBiotech, 0100–20). The F-actin of cells was stained with TRITC-phalloidin (Sigma). The cell nuclei were counterstained with DAPI Fluoromount-G mounting medium. Immunofluorescence photographs were captured using an Olympus IX83 inverted microscope and processed with Olympus CellSens™ Microscope Imaging Software.

Mitochondria isolation

A mitochondria isolation kit (QIAGEN, 37612) was used to isolate mitochondria. Approximately 5×10^6 to 2×10^7 cells were collected and centrifuged at 500 × g for 10 min at 4°C. Then, the cell pellets were resuspended in 1 ml ($<1 \times 10^7$ cells) or 2 ml ($\geq 1 \times 10^7$ cells) ice-cold lysis buffer and incubated in an end-over-end shaker for 10 min on ice. The cell lysates were centrifuged at 1000 × g at 4°C for 10 min and the supernatants were removed. The cell pellets were resuspended in 1.5 ml ice-cold disruption buffer. The cell lysates were centrifuged at 1000 × g at 4°C for 10 min. The supernatants were centrifuged at 6000 × g at 4°C for 10 min and the supernatants were removed. The pellets containing mitochondria were resuspended in 100 µl of storage buffer.

Extraction of cytoplasmic and nuclear proteins

For the extraction of cytoplasmic and nuclear proteins, we used the Nuclear and Cytoplasmic Extraction Kit (CWBIO Cat. #CW0199S) according to the manufacturer's protocol.

Measurement of glutamic acid and ammonia

Cells were cultured in 100 mm dishes in RPMI 1640 supplemented with 10% FBS. The supernatants were collected, and the cell pellets were ultrasonically lysed using an Ultrasonic Processor (Qsonica). For glutamic acid measurement, we used the Glutamic Acid Measurement Kit (Nanjing Jiancheng Bioengineering Institute, Cat. #A074) according to the manufacturer's protocol. For ammonia measurement, we used the Blood Ammonia Assay Kit (Nanjing Jiancheng Bioengineering Institute, Cat. #A086) according to the manufacturer's protocol.

Statistical analysis

All experiments were performed in triplicate. All the data were expressed as the mean ± SD. ANOVA, and paired t-tests were used to make statistical comparisons. $P < 0.05$ was considered to be statistically significant.

Results

APC10 is overexpressed in NSCLC cell lines and located in the cytoplasm

Lung cancer is the most common cancer worldwide. Based on tumor histology, lung cancer is classified as small cell lung cancer (SCLC) and NSCLC [38]. Compared to SCLC patients, the response of NSCLC patients to radiation and chemotherapy is inefficient [39]. Thus, NSCLC treatment urgently needs a new, more effective therapeutic strategy. Until now, little has been known about the functions of APC10 in NSCLC cells. We first examined the expression of APC10 protein levels in NSCLC tissue samples. The protein levels of APC10 in NSCLC tissues were high compared to those in adjacent normal tissues (Figure 1(a,b)). To profile the expression pattern of APC10 in NSCLC cell lines, we used five NSCLC cell lines (A549, H1299, H358, H292 and SPC-A1) and two normal human bronchial epithelial cell cultures (HBE and Beas-2b) to detect the expression of APC10. Figure 1(c) shows that APC10 protein levels were significantly higher in NSCLC cell lines than in HBE and Beas-2b cells. The location of APC10 in NSCLC cells is unclear. In an effort to profile the location of APC10 in

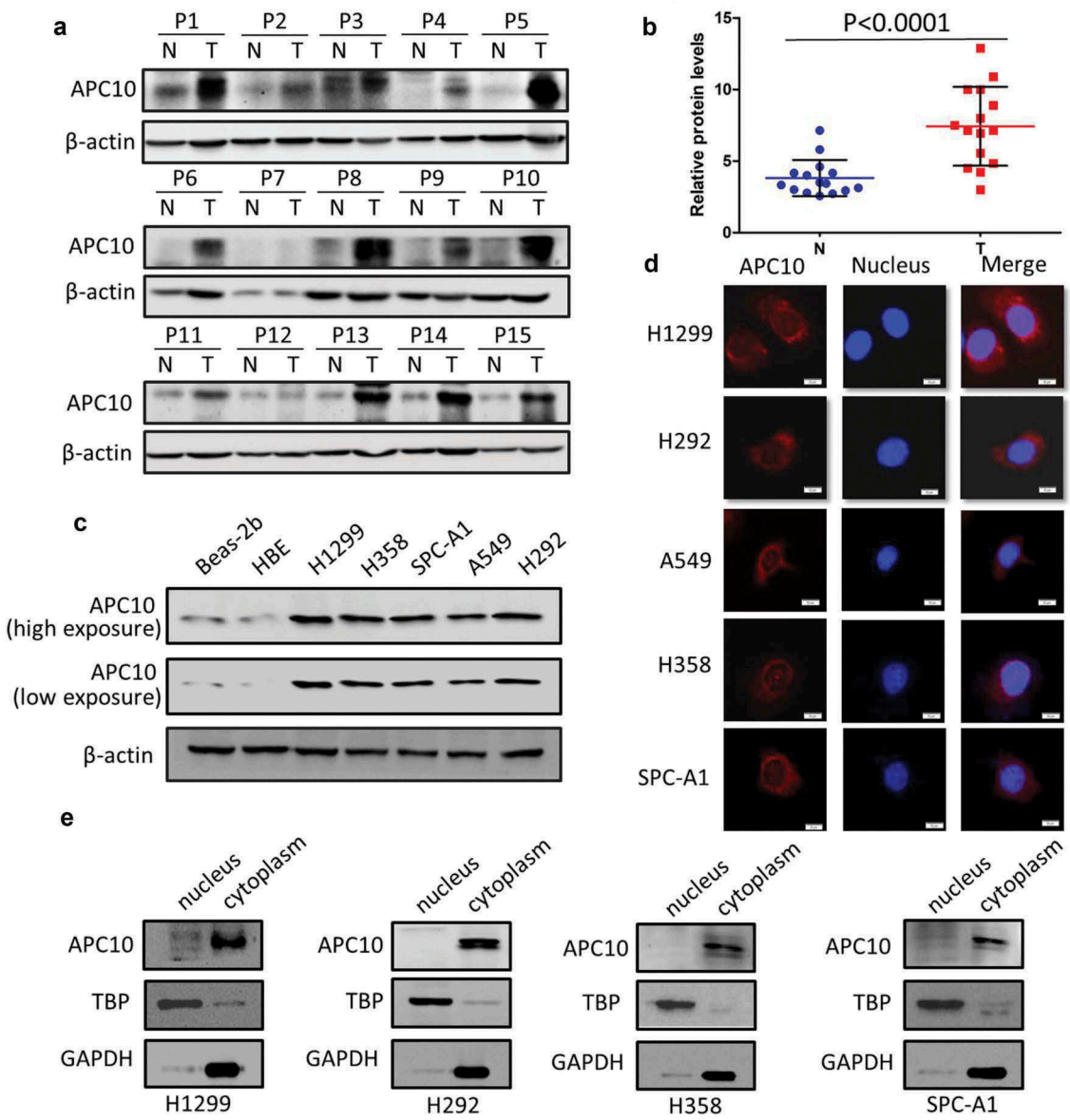

Figure 1. APC10 is overexpressed in non-small cell lung cancer and located in the cytoplasm. (a) The protein levels of APC10 were determined by western blot using the paired, tumor-adjacent noncancerous lung tissues (normal, N) and human NSCLC tissues (tumor, T) from 15 NSCLC patients (P1 – P15). (b) The expression of APC10 was quantified in these normal and tumor tissues. The p value was calculated by paired t test. (c) The protein levels of APC10 in two normal lung cell cultures (Beas-2b and HBE) and five NSCLC cell lines (H1299, H358, SPC-A1, A549 and H292) were detected by western blot. (d) The location of APC10 was detected by immunofluorescence staining in five NSCLC cell lines (H1299, H292, A549, H358 and SPC-A1). Cells were stained with anti-APC10 (left panel, red) and DAPI (middle panel, blue). The merged images are shown in the right panel. Scale bar = 50 μm, magnification: 200 × . (e) The nuclear and cytoplasmic fractions were separated and the location of APC10 was detected by western blot in H1299, H292, H358 and SPC-A1 cells. TBP: TATA binding protein, GAPDH: glyceraldehyde-3-phosphate dehydrogenase.

NSCLC cell lines, we performed immunofluorescence staining and found that APC10 was located in the cytoplasm, especially in the perinuclear area (Figure 1(d)). Next, we separated the cytoplasmic proteins from nuclear proteins. Western blot indicated that APC10 was located in the cytoplasm (Figure 1(e)).

APC10 promotes the proliferation of NSCLC cells

We next examined the functions of APC10 in NSCLC cells. The proliferation of NSCLC cells was detected by crystal violet staining. As shown in Figure 2(a), APC10 knockdown dramatically retarded the growth of H1299 and H292 cells. To further confirm the effect, we cotransfected cells

with APC10 siRNAs and a mutant APC10 plasmid that resists APC10 siRNA mediated gene silencing. We found that the growth caused by APC10 knockdown was restored in H1299 and H292 cells (Figure 2(b)). Similar results were obtained in a colony formation assay. The APC10 knockdown significantly decreased colony formation by H1299 and H292 cells (Figure 2(c)). Further, we overexpressed APC10 in A549 cells. A saturation density assay indicated that overexpression of APC10 promoted the growth of A549 (Figure 2(d)).

APC10 knockdown inhibits the migration of NSCLC cells

We next assessed the possible effects of APC10 on the migration of NSCLC cells. A wound healing assay was performed and showed that the migration rate was markedly attenuated when H1299 and H292 cells were transfected with APC10 siRNAs (Figure 3(a,b)). To further confirm the effect, a transwell assay was performed. The result showed that the number of migrated cells was reduced when H1299 cells were transfected with APC10 siRNAs (Figure 3(c)). An F-actin staining assay also showed that the number of pseudopodia was greatly reduced when APC10 was knocked down in H1299 cells (Figure 3(d)).

APC10 knockdown arrests the cell cycle in the G0/G1 phase

A previous study indicated that APC/C inhibition induced a cell cycle arrest in metaphase and

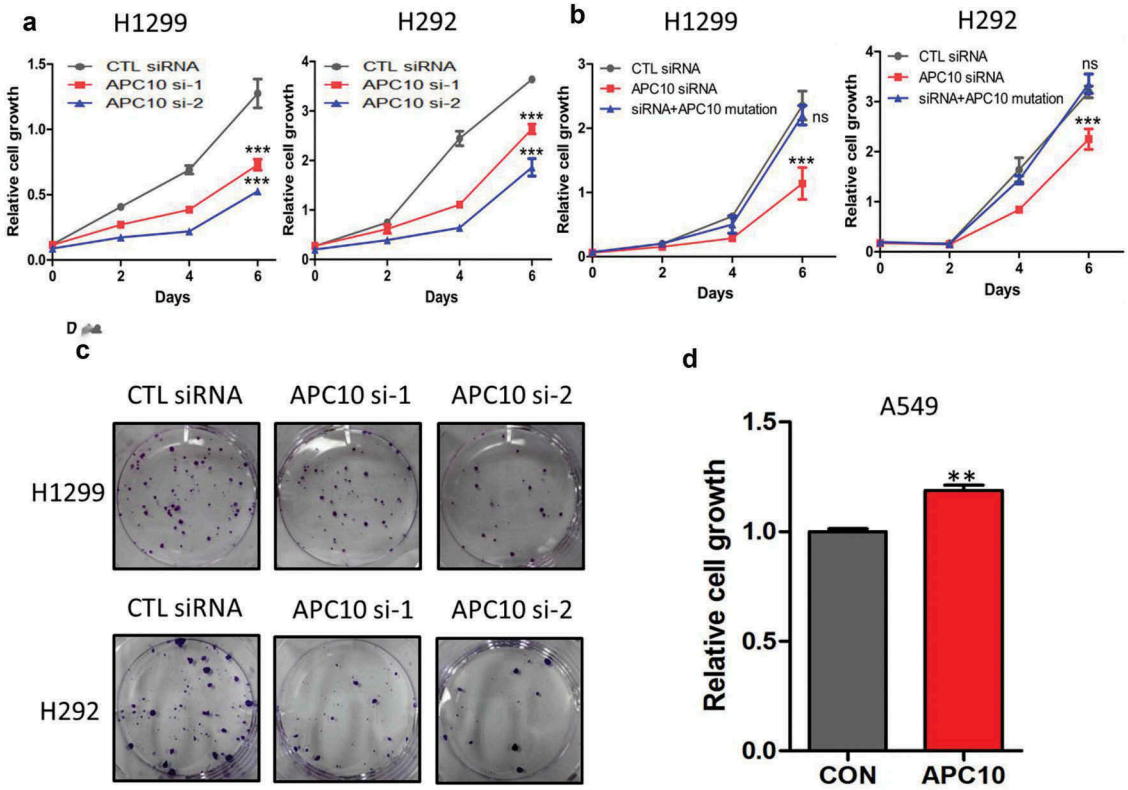

Figure 2. APC10 promotes the proliferation of NSCLC cells. (a, b) H1299 and H292 cells were transfected with control (CTL) siRNAs or APC10 siRNAs (a). H1299 and H292 cells were cotransfected with APC10 siRNAs and a mutant APC10 plasmid that resists APC10 siRNA mediated gene silencing (b). Cells were trypsinized, counted and seeded in 24-well plates with 3000 cells per well. At the indicated times, cells were fixed and stained with crystal violet. Dye was extracted and detected via absorbance at 595 nm wavelength. The data represent the averages of three independent experiments (mean ± SD). ***P < 0.001, ns: P > 0.05. (c) Colony formation assay. H1299 and H292 cells were transfected with either control siRNA or APC10 siRNAs. Cells were trypsinized, counted and seeded in 6-well plates with 500 cells per well. After 10 days, cells were fixed and stained with crystal violet. Representative wells were photographed and shown. (d) Saturation density assay. A549 cells were transfected with HA-APC10. Cells were trypsinized, counted and seeded in 12-well plates. After 6 days, cells were trypsinized and counted. The data represent the averages of three independent experiments (mean ± SD). **P < 0.01.

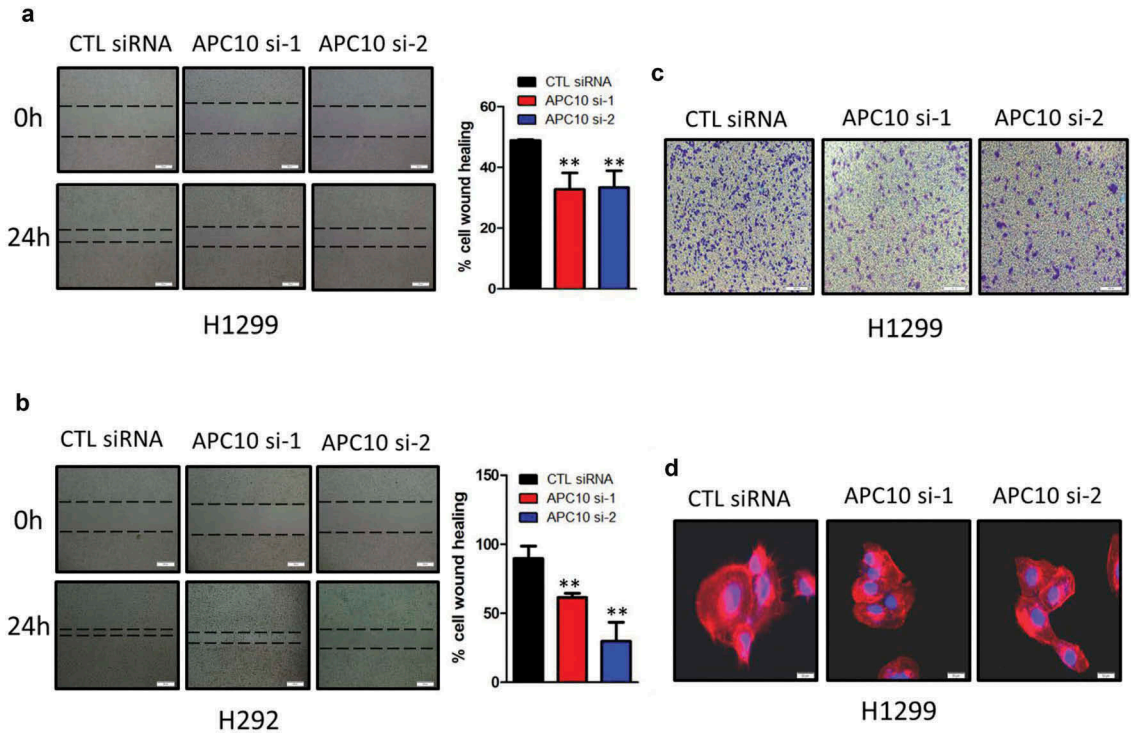

Figure 3. The knockdown of APC10 inhibits the migration of NSCLC cells. (a, b) Scratch wound healing assay. H1299 and H292 cells were transfected with either control (CTL) siRNA or APC10 siRNAs. The extent of cell migration was photographed at the indicated times (Olympus, IX71, scale bar = 200 μm, magnification: 100×) (left). The transverse scratch wounds were re-examined and analyzed using ImageJ software at different sites from each wound area at each time point. The results are presented as the mean ± SD (right). **P < 0.01. (c) Transwell migration assay. H1299 cells were transfected with either control siRNA or APC10 siRNAs. Cells were trypsinized, counted and seeded in transwell chambers at 24 h after transfection. After incubation for 10 h, the cells were fixed, stained and photographed (scale bar = 200 μm, magnification: 100×). (d) F-actin staining assay. H1299 cells were transfected with either control siRNA or APC10 siRNAs. After 48 h, cells were stained with DAPI as a nuclear marker and phalloidin. The merged images are shown (scale bar = 50 μm, magnification: 200×).

resulted in the accumulation of the APC/C substrate, Cyclin B1 [29]. We next detected the effects of APC10 knockdown on cell cycle progression. First, we blocked H1299 cells in early mitosis following a synchronization protocol by thymidine and nocodazole (Thy-Noc) treatment [37]. Then, cells were transfected with APC10 siRNAs. After 24 h, we detected the effects of APC10 knockdown on cell cycle progression by flow cytometry. As seen in Figure 4(a,b), knockdown of APC10 induced cell cycle arrest in the G0/G1 phase. This result was in contrast to the conventional conception that APC/C inhibition induces cell cycle arrest in metaphase. We further examined the protein levels (Figure 4(c)) of cell cycle-related genes in H1299 cells with APC10 knockdown and found that the protein expression patterns were consistent with the cell cycle analysis. CDC25A is required for progression from G1 to the S phase of the cell cycle, and it was downregulated. CDC25C, CDK1 and Cyclin B1 play roles in the G2/M phase. Because the cell G2/M phase was reduced, they were downregulated. RB1, as a negative regulator of the cell cycle, prevents cells from passing through the G1-S checkpoint, so RB1 was upregulated. Importantly, the protein levels of Cyclin B1 were clearly decreased that were statistically significant (Figure 4(c,d)). To further confirm the effect, we cotransfected APC10 siRNAs and a mutant APC10 plasmid that resists APC10 siRNA mediated gene silencing. We found that the protein levels of Cyclin B1 caused by APC10 knockdown were restored in H1299 cells (Figure 4(e)). The mRNA levels of cell cycle-related genes in H1299 cells with APC10 knockdown were consistent with the cell cycle analysis (Supplemental Figure S1(a)). The mRNA levels of Cyclin B1 were also decreased when APC10 was knocked down. This further confirmed that APC10 inhibition reduced, rather

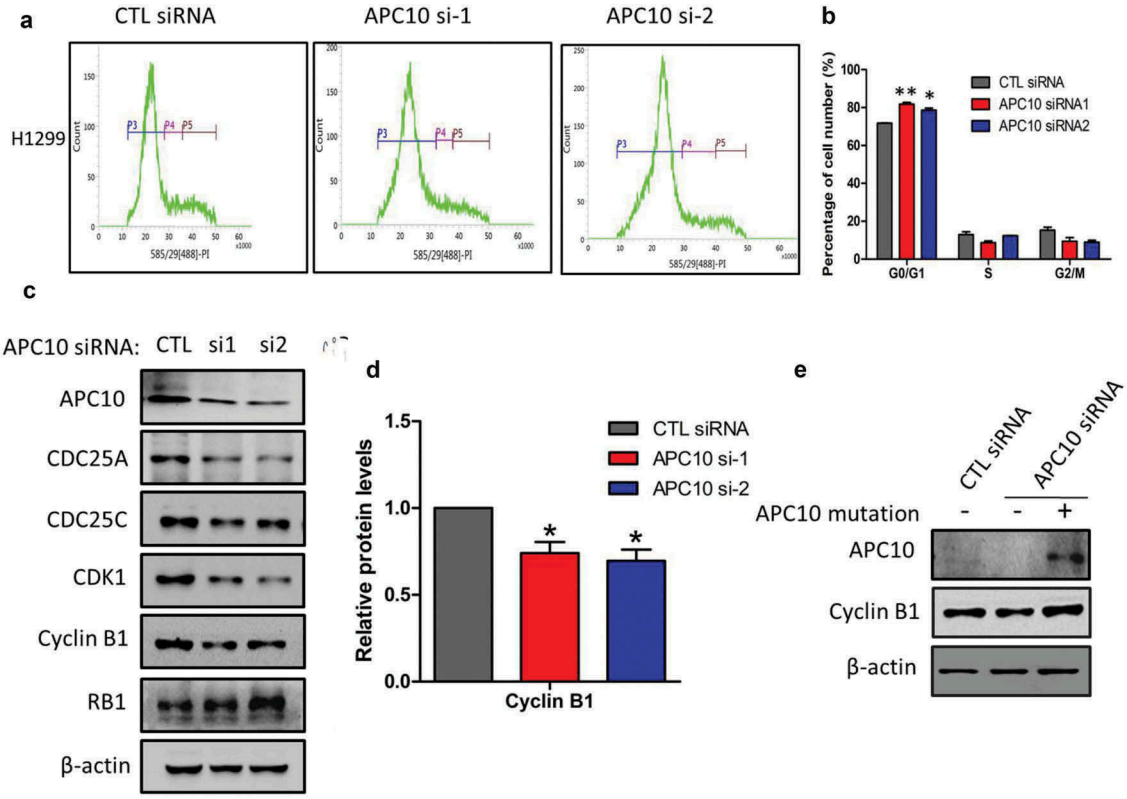

Figure 4. The knockdown of APC10 arrests cell cycle at the G0/G1 phase. (a, b) H1299 cells were synchronized in early mitosis. Cells were then transfected with either control (CTL) siRNA or APC10 siRNAs. After 24 h, cell cycle analysis was done by flow cytometry (A). The inserts show the quantification of the cell cycle analysis. The data represent the averages of three independent experiments (mean ± SD). *P < 0.05, **P < 0.01 (b). (c) H1299 cells were transfected with either control siRNA or APC10 siRNAs. The protein levels of cell cycle related proteins were checked by western blot. (d) The protein levels of Cyclin B1 were quantified by gray analysis. The results are presented as the mean ± SD. *P < 0.05. (e) H1299 cells were cotransfected with APC10 siRNAs and a mutant APC10 plasmid that resists APC10 siRNA mediated gene silencing. The expression of Cyclin B1 was analyzed by western blot.

than increased, the expression of the APC/C substrate, Cyclin B1. Therefore, these intriguing results suggested that APC10 might possess new functions independent of APC/C.

APC10 knockdown downregulates glutaminolysis by decreasing GAC

We demonstrated that APC10 is located in the cytoplasm (Figure 1(d,e)). To figure out the precise molecular mechanism of APC10 in NSCLC, we performed immunofluorescence staining using markers specific for organelles in H1299 cells. We found that the location of APC10 overlapped with the marker specific for mitochondria (Figure 5(a)), indicating that APC10 is located at the mitochondria. To further confirm the result, we separated the mitochondria and microsomal fraction (endoplasmic reticulum and plasma membrane) from the cytosol of H1299 and H292 cells. Western blotting indicated that APC10 was only located in mitochondria (Figure 5(b)). GAC is the key enzyme in glutaminolysis, and GAC is located in mitochondria [40]. In our previous study, we demonstrated that GAC played an important role in the proliferation and tumorigenesis of NSCLC [41]. We wondered if APC10 could affect glutaminolysis. Figure 5(c,d) show that APC10 coimmunoprecipitated with GAC. To confirm that the interaction between APC10 and GAC was independent of the APC/C or other APC/C subunits, we examined the interaction of GAC with other APC/C subunits. Anaphase promoting complex subunit 2 (APC2), which binds to APC10, constitutes the catalytic module of the APC/C. APC2 is a core APC/C subunit involved in the substrate recognition step and poly-ubiquitin chain extension [42]. Cell division cycle protein 27 homologue (CDC27) is also a core APC/C subunit involved in binding to substrates and cofactors [43]. Therefore, we tested if

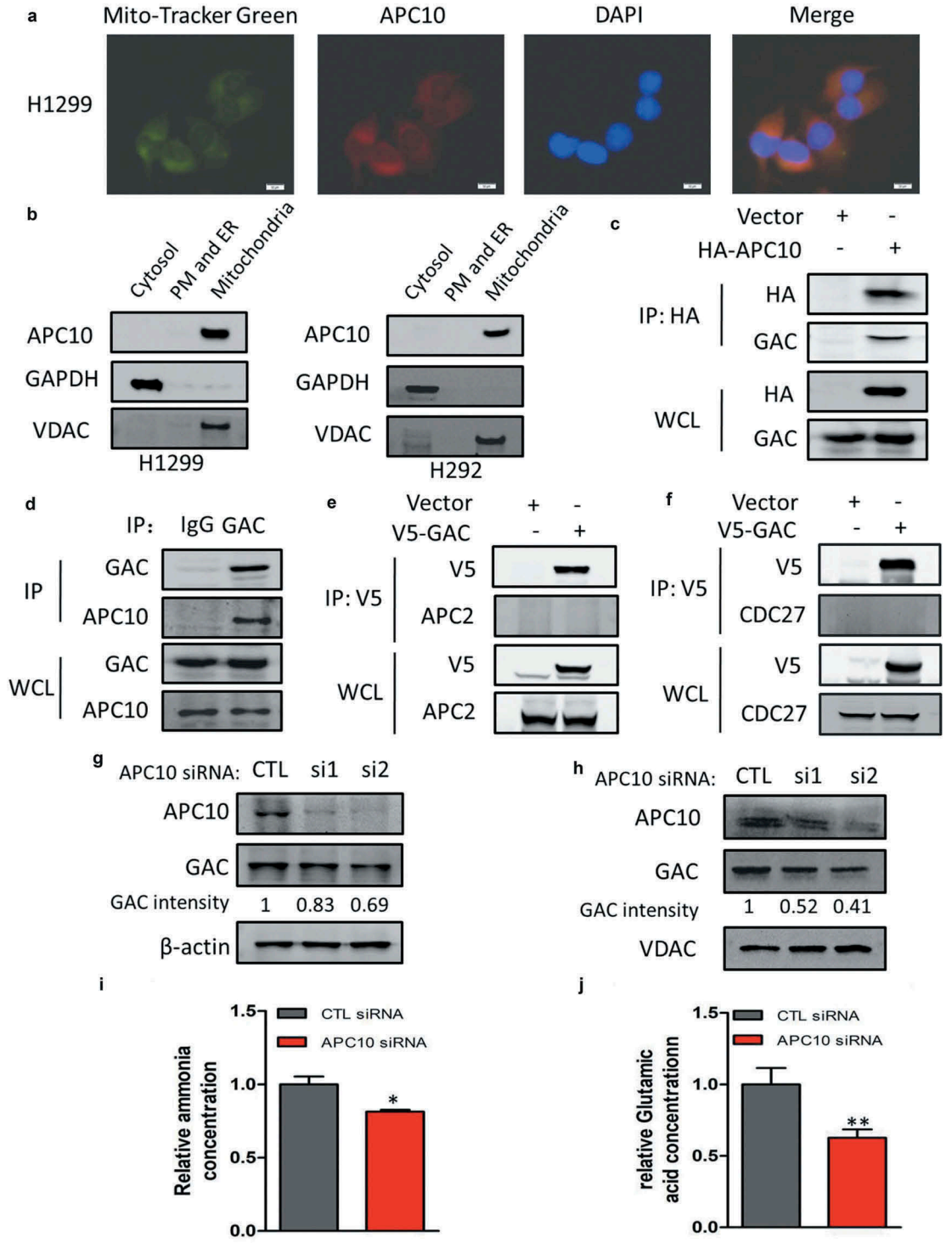

Figure 5. The knockdown of APC10 downregulates glutaminolysis by decreasing GAC. (a) The subcellular location of endogenous APC10 was detected by immunofluorescence staining in H1299 cells. Cells were stained with Mito-Tracker Green (green), anti-APC10 (red) and DAPI (blue). The merged image is shown in the right panel. Scale bar = 50 μm, magnification: 200 ×. (b) Cytosol, PM (plasma membrane) and ER (endoplasmic reticulum), and mitochondria were separated, and the location of APC10 was detected by western blot in H1299 and H292 cells. (c) H1299 cells were transiently transfected with a plasmid expressing HA-APC10. The immunoprecipitates were blotted with anti-HA or anti-GAC antibodies. WCL: the whole cell lysate. (d) The immunoprecipitates of H1299 cells were blotted with anti-GAC or anti-APC10 antibodies. (E, F) H1299 cells were transiently transfected with a plasmid expressing V5-GAC. The immunoprecipitates of the H1299 cells were blotted with anti-V5 and anti-APC2 (E) or anti-CDC27 (f) antibodies. (g) H1299 cells were transfected with either control (CTL) siRNA or APC10 siRNAs. After 48 h, the protein levels of GAC were detected by western blot. The GAC intensity was calculated by normalizing against β-actin. (h) H1299 cells were transfected with either control siRNA or APC10 siRNAs. After 48 h, mitochondria were isolated. The protein levels of GAC in the mitochondria were detected by western blot. The GAC intensity was calculated by normalizing against voltage dependent anion channel (VDAC). (i, j) H1299 cells were transfected with either control siRNA or APC10 siRNAs. After 48 h, cells were collected and ultrasonically lysed. The relative concentrations of ammonia (i) and glutamic acid (j) were detected. The data represent the averages of three independent experiments (mean ± SD). *P < 0.05, **P < 0.01.

APC2 or CDC27 could interact with GAC. Figure 5 (e,f) show that APC2 and CDC27 could not interact with GAC. These results indicated that the interaction between APC10 and GAC was independent of APC/C. We next examined the effects of APC10 on the expression of GAC. Figure 5(g,h) show that knocking down APC10 reduced the expression of GAC. Glutaminase is known to catalyze the formation of glutamate and ammonia from glutamine. We therefore examined the effects of APC10 on glutamine metabolism by measuring the concentration of ammonia and glutamate in H1299 cells. Figure 5(i,j) show that the concentrations of ammonia and glutamate in APC10 knockdown cells were less than those in control cells. These findings demonstrated that APC10 regulated glutamine metabolism through interaction with GAC.

APC10 knockdown induces autophagy by downregulating glutamine metabolism

A previous study indicated that mTORC1 signaling is repressed to activate autophagy when the conversion of glutamine to glutamate is abolished [15]. This finding led us to explore if APC10 could affect autophagy. During autophagy, microtubule-associated protein 1 light chain 3 (LC3) is cleaved to form LC3-I. LC3-I is easily activated and conjugated to the amino group of phosphatidylethanolamine and bound to the autophagosome membrane to form LC3-II (autophagy guideline). This can be detected by observing the shift in molecular weight on immunoblots. As shown in Figure 6(a), we transfected APC10 siRNAs into H1299 cells stably expressing microtubule-associated protein 1 light chain 3 fused with green fluorescent protein (GFP-LC3B). The LC3B puncta were significantly increased when APC10 was knocked down. We further assessed the expression levels of LC3-I/II in H1299 cells (Figure 6(b)). APC10 knockdown decreased the expression of LC3-II; however, lysosome inhibition by CQ increased the LC3-II level in APC10 knockdown cells compared with that in control cells. These data indicated that APC10 knockdown induced autophagy and increased the autophagic flux. To elucidate if the autophagy induced by APC10 knockdown was caused by the reduced GAC level, we overexpressed GAC when APC10 was knocked down, and then detected the LC3-II level. Figure 6(c) shows that overexpressing GAC could recover the reduced expression of LC3-II caused by APC10 knockdown. This result indicated that the autophagy induced by APC10 knockdown was caused by the disturbance of glutamine metabolism. To confirm whether APC10 induced autophagy by mTORC1-ULK1 signaling, we assessed the protein levels of phosphor-ULK1 (S758) and total ULK1. As shown in Figure 6(d), knockdown of APC10 caused a progressive reduction of phosphor-ULK1. This indicated that ULK1 was activated and autophagy was induced. In cancer, autophagy plays a dual role, either functioning as a tumor suppressor or promoting tumor progression [4]. To confirm the role of autophagy induced by knockdown of APC10, we added the autophagy inhibitor CQ to H1299 cells with APC10 knockdown and performed an MTT assay (Figure 6(e)). We found that the growth caused by APC10 knockdown was restored in H1299 cells treated with CQ compared with that in control cells. Collectively, these data revealed that APC10 knockdown induced autophagy by decreasing GAC and downregulating glutamine metabolism.

Discussion

The APC/C is a cell cycle-regulated multimeric E3 ubiquitin ligase [16,17]. During mitosis and G1 phase of the cell cycle, the APC/C is activated to regulate the transition from metaphase to anaphase and the exit from mitosis [20–22]. In recent years, the APC/C has been reported to play new cell cycle-independent functions in nonmitotic cells and specifically in neuronal structure and function [44]. APC10 is a core subunit of APC/C. Previous studies have reported that APC10 plays a critical role in substrate recognition and APC/C ubiquitination activity [32–36]. These studies indicated that APC10 plays an indispensable role as an APC/C subunit when the APC/C exerts its function normally. However, the role of APC10 independent of the APC/C has not been studied yet. In this study, we focused on a new role of APC10 independent of the APC/C in NSCLC cells. We discovered that APC10 is overexpressed in NSCLC cell lines and located in the cytoplasm. We further characterized the biological functions

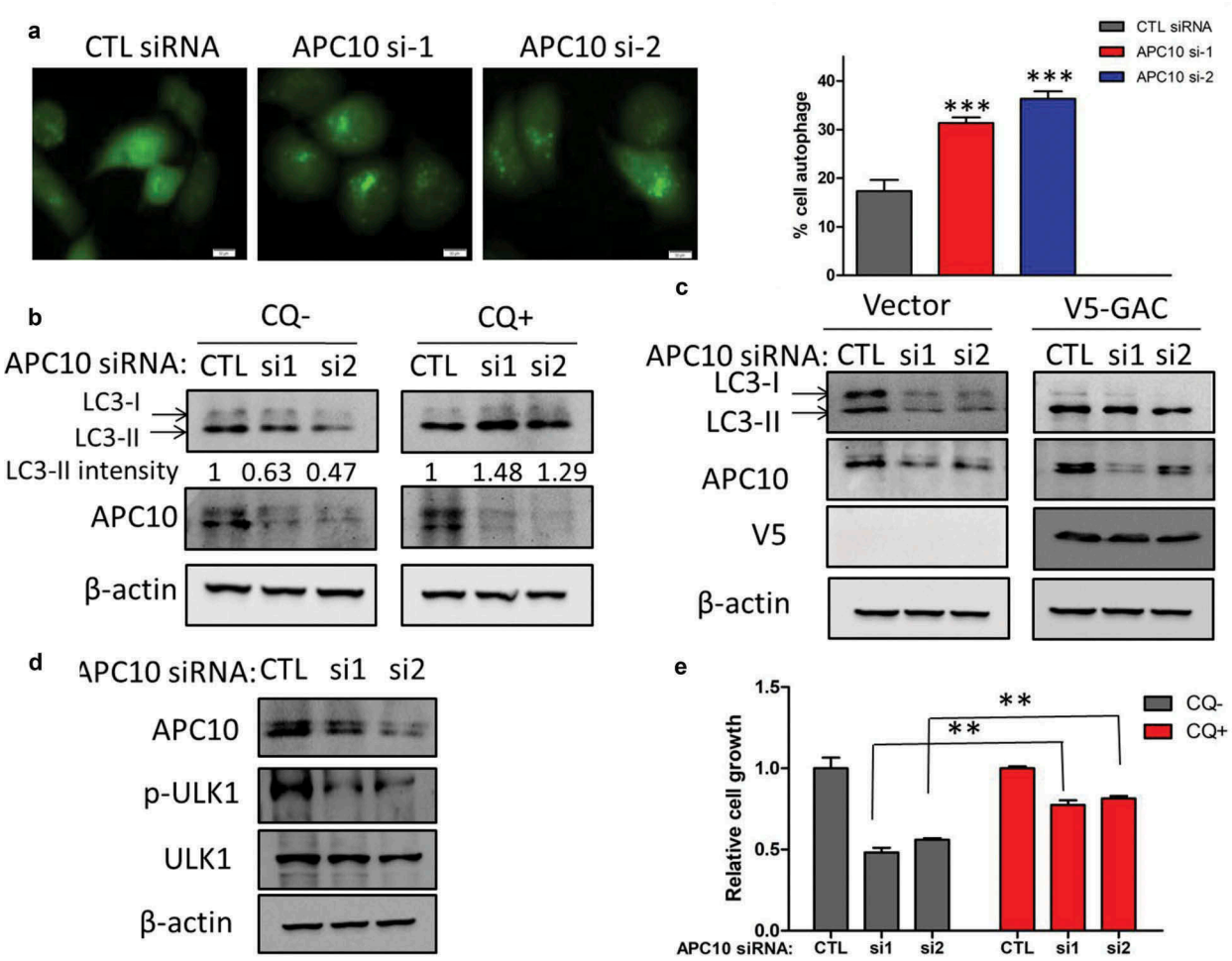

Figure 6. APC10 knockdown induces autophagy by downregulating glutamine metabolism. (a) H1299 cells stably expressing GFP-LC3B were transfected with either control (CTL) siRNA or APC10 siRNAs and cultured for 48 h. Cells were photographed with fluorescence microscopy (Olympus, IX71, scale bar = 50 μm, magnification: 200×) (left). The number of cells with GFP-LC3B puncta was counted and analyzed using the image-pro program. ***P < 0.001 (right). (b) H1299 cells stably expressing GFP-LC3B were transfected with either control siRNA or APC10 siRNAs and treated or not treated with CQ. The expression of LC3 was analyzed by western blot. The LC3-II intensity was calculated by normalizing against β-actin. (c) H1299 cells were cotransfected with the indicated siRNAs and V5-GAC plasmid or vector. The expression of LC3 was analyzed by western blot. (d) H1299 cells were transfected with either control siRNA or APC10 siRNAs. The protein levels of phosphor-ULK1 (p-ULK1 [S758]) and total ULK1 were detected by western blot. (e) H1299 cells were transfected with the indicated siRNAs and treated or not treated with CQ. The MTT assay was used to assess the growth rate. The data represent the averages of three independent experiments (mean ± SD). **P < 0.01.

of APC10 in the proliferation and migration of NSCLC cells. The knockdown of APC10 significantly inhibited the proliferation and migration of NSCLC cells, and overexpressing APC10 promoted the proliferation of A549 cells. A previous study reported that APC/C inhibition induced a cell cycle arrest in metaphase and resulted in the accumulation of the APC/C substrate, Cyclin B1 [29]. However, we performed flow cytometry to analyze the cell cycle and found that APC10 knockdown arrested the cell cycle in the G0/G1 phase, not metaphase. We also detected the protein levels of the APC/C substrate, Cyclin B1, and found that the protein levels of Cyclin B1 were reduced, not increased. These results indicated that APC10 might possess a new role in NSCLC cells independent of the APC/C. GAC, the first and the rate-limiting enzyme in glutamine metabolism, is involved in cancer initiation and progression [12–14]. We found that APC10 could interact with GAC. The knockdown of APC10 decreased GAC protein levels and downregulated glutamine metabolism. As a consequence, the conversion of glutamine to glutamate was abolished.

This further led to the induction of autophagy through inhibition of the mTORC1-ULK1 axis.

In conclusion, we discovered a new role of APC10 in NSCLC cells that was independent of APC/C. We proved that APC10 was overexpressed in NSCLC cells and patient tissues; such overexpression might be a promising biomarker for the diagnosis of NSCLC. We also found that APC10 was a potential regulator for the proliferation and migration of NSCLC cells. The molecular mechanism was found to be the regulation of glutamine metabolism by APC10 through interaction with GAC, which induces autophagy. This function of APC10 was independent of APC/C. However, the precise mechanism by which APC10 regulates GAC is still not clear. The changes of GAC expression level caused by APC10 may be the effect of ubiquitination. Therefore, we will investigate the precise mechanisms of how APC10 regulates GAC in the next step. Regardless, our study, for the first time, connected a cell cycle-related protein to glutamine metabolism, and this work may shed new light on exploring the regulatory mechanisms of cancer metabolism.

Disclosure statement

No potential conflict of interest was reported by the authors.

Funding

This work is supported by grants to J-B Wang from the National Natural Science Foundation of China [81372823, 31360282] and a grant from the Department of Education of Jiangxi Province [701, Science and Technology Luo Di program].

ORCID

Caifeng Xie http://orcid.org/0000-0002-0903-638X

References

[1] Mizushima N. Autophagy: process and function. Genes Dev. 2007;21(22):2861–2873.
[2] Xie Z, Klionsky DJ. Autophagosome formation: core machinery and adaptations. Nat Cell Biol. 2007;9(10):1102–1109.
[3] Scott SV, Klionsky DJ. Delivery of proteins and organelles to the vacuole from the cytoplasm. Curr Opin Cell Biol. 1998;10(4):523–529.
[4] Zhi X, Zhong Q. Autophagy in cancer. F1000Prime Rep. 2015;7:18.
[5] Ganley IG, Lam DH, Wang J, et al. ULK1.ATG13.FIP200 complex mediates mTOR signaling and is essential for autophagy. J Biol Chem. 2009;284(18):12297–12305.
[6] Hosokawa N, Hara T, Kaizuka T, et al. Nutrient-dependent mTORC1 association with the ULK1-Atg13-FIP200 complex required for autophagy. Mol Biol Cell. 2009;20(7):1981–1991.
[7] Jung CH, Jun CB, Ro S-H, et al. ULK-Atg13-FIP200 complexes mediate mTOR signaling to the autophagy machinery. Mol Biol Cell. 2009;20(7):1992–2003.
[8] Jewell JL, Russell RC, Guan KL. Amino acid signalling upstream of mTOR. Nat Rev Mol Cell Biol. 2013;14(3):133–139.
[9] Kanazawa T, Taneike I, Akaishi R, et al. Amino acids and insulin control autophagic proteolysis through different signaling pathways in relation to mTOR in isolated rat hepatocytes. J Biol Chem. 2004;279(9):8452–8459.
[10] Kuma A, Hatano M, Matsui M, et al. The role of autophagy during the early neonatal starvation period. Nature. 2004;432(7020):1032–1036.
[11] Lin TC, Chen Y-R, Kensicki E, et al. Autophagy: resetting glutamine-dependent metabolism and oxygen consumption. Autophagy. 2012;8(10):1477–1493.
[12] Gao P, Tchernyshyov I, Chang T-C, et al. c-Myc suppression of miR-23a/b enhances mitochondrial glutaminase expression and glutamine metabolism. Nature. 2009;458(7239):762–765.
[13] Wang JB, Erickson JW, Fuji R, et al. Targeting mitochondrial glutaminase activity inhibits oncogenic transformation. Cancer Cell. 2010;18(3):207–219.
[14] van Den Heuvel AP, Jing J, Wooster RF, et al. Analysis of glutamine dependency in non-small cell lung cancer: GLS1 splice variant GAC is essential for cancer cell growth. Cancer Biol Ther. 2012;13(12):1185–1194.
[15] Tan HWS, Sim AYL, Long YC. Glutamine metabolism regulates autophagy-dependent mTORC1 reactivation during amino acid starvation. Nat Commun. 2017;8(1):338.
[16] Irniger S, Piatti S, Michaelis C, et al. Genes involved in sister chromatid separation are needed for B-type cyclin proteolysis in budding yeast. Cell. 1995;81(2):269–78.
[17] Sudakin V, Ganoth D, Dahan A, et al. The cyclosome, a large complex containing cyclin-selective ubiquitin ligase activity, targets cyclins for destruction at the end of mitosis. Mol Biol Cell. 1995;6(2):185–97.
[18] Thornton BR, Toczyski DP. Precise destruction: an emerging picture of the APC. Genes Dev. 2006;20(22):3069–78.

[19] Peters JM. The anaphase promoting complex/cyclosome: a machine designed to destroy. Nat Rev Mol Cell Biol. 2006;7(9):644–56.
[20] Zachariae W, Nasmyth K. Whose end is destruction: cell division and the anaphase-promoting complex. Genes Dev. 1999;13(16):2039–58.
[21] Harper JW, Burton JL, Solomon MJ. The anaphase-promoting complex: it's not just for mitosis any more. Genes Dev. 2002;16(17):2179–206.
[22] Peters JM. The anaphase-promoting complex: proteolysis in mitosis and beyond. Mol Cell. 2002;9(5):931–43.
[23] Kim AH, Puram SV, Bilimoria PM, et al. A centrosomal Cdc20-APC pathway controls dendrite morphogenesis in postmitotic neurons. Cell. 2009;136(2):322–36.
[24] Herrero-Mendez A, Almeida A, Fernández E, et al. The bioenergetic and antioxidant status of neurons is controlled by continuous degradation of a key glycolytic enzyme by APC/C-Cdh1. Nat Cell Biol. 2009;11(6):747–52.
[25] Manchado E, Guillamot M, de Cárcer G, et al. Targeting mitotic exit leads to tumor regression in vivo: modulation by Cdk1, Mastl, and the PP2A/B55alpha,delta phosphatase. Cancer Cell. 2010;18(6):641–54.
[26] Smolders L, Teodoro JG. Targeting the anaphase promoting complex: common pathways for viral infection and cancer therapy. Expert Opin Ther Targets. 2011;15(6):767–80.
[27] Sackton KL, Dimova N, Zeng X, et al. Synergistic blockade of mitotic exit by two chemical inhibitors of the APC/C. Nature. 2014;514(7524):646–9.
[28] WangL, Zhang J, Wan L, et al. Targeting Cdc20 as a novel cancer therapeutic strategy. Pharmacol Ther. 2015;151:141–51.
[29] Lub S, Maes A, Maes K, et al. Inhibiting the anaphase promoting complex/cyclosome induces a metaphase arrest and cell death in multiple myeloma cells. Oncotarget. 2016;7(4):4062–76.
[30] Eguren M, Porlan E, Manchado E, et al. The APC/C cofactor Cdh1 prevents replicative stress and p53-dependent cell death in neural progenitors. Nat Commun. 2013;4:2880.
[31] Grossberger R, Gieffers C, Zachariae W, et al. Characterization of the DOC1/APC10 subunit of the yeast and the human anaphase-promoting complex. J Biol Chem. 1999;274(20):14500–7.
[32] Kominami K, Seth-Smith H, Toda T. Apc10 and Ste9/Srw1, two regulators of the APC-cyclosome, as well as the CDK inhibitor Rum1 are required for G1 cell-cycle arrest in fission yeast. Embo J. 1998;17(18):5388–5399.
[33] Kurasawa Y, Todokoro K. Identification of human APC10/Doc1 as a subunit of anaphase promoting complex. Oncogene. 1999;18(37):5131–5137.
[34] Carroll CW, Morgan DO. The Doc1 subunit is a processivity factor for the anaphase-promoting complex. Nat Cell Biol. 2002;4(11):880–887.
[35] Passmore LA, McCormack EA, Au SWN, et al. Doc1 mediates the activity of the anaphase-promoting complex by contributing to substrate recognition. Embo J. 2003;22(4):786–796.
[36] Carroll CW, Enquist-Newman M, Morgan DO. The APC subunit Doc1 promotes recognition of the substrate destruction box. Curr Biol. 2005;15(1):11–18.
[37] Apraiz A, Mitxelena J, Zubiaga A. Studying cell cycle-regulated gene expression by two complementary cell synchronization protocols. J Vis Exp. 2017;(124):e55745.
[38] Devesa SS, Bray F, Vizcaino AP, et al. International lung cancer trends by histologic type: male:female differences diminishing and adenocarcinoma rates rising. Int J Cancer. 2005;117(2):294–299.
[39] Johnson DH, Schiller JH, Bunn PA Jr. Recent clinical advances in lung cancer management. J Clin Oncol. 2014;32(10):973–982.
[40] Cassago A, Ferreira APS, Ferreira IM, et al. Mitochondrial localization and structure-based phosphate activation mechanism of Glutaminase C with implications for cancer metabolism. Proc Natl Acad Sci U S A. 2012;109(4):1092–1097.
[41] Han T, Zhan W, Gan M, et al. Phosphorylation of glutaminase by PKCepsilon is essential for its enzymatic activity and critically contributes to tumorigenesis. Cell Res. 2018;28(6):655–669.
[42] Marrocco K, Criqui M-C, Zervudacki J, et al. APC/C-mediated degradation of dsRNA-binding protein 4 (DRB4) involved in RNA silencing. PLoS One. 2012;7(4):e35173.
[43] Primorac I, Musacchio A. Panta rhei: the APC/C at steady state. J Cell Biol. 2013;201(2):177–189.
[44] Manchado E, Eguren M, Malumbres M. The anaphase-promoting complex/cyclosome (APC/C): cell-cycle-dependent and -independent functions. Biochem Soc Trans. 2010;38(Pt 1):65–71.